Single electron–photon logic device using coupled quantum dots: Computation with the Fock ground state

K. Nomoto,[a] R. Ugajin, T. Suzuki, and I. Hase
Sony Corporation Research Center, 174 Fujitsuka-cho, Hodogaya-ku, Yokohama 240, Japan

(Received 14 August 1995; accepted for publication 12 September 1995)

We propose a novel logic device using coupled quantum dots (CQDs) in which single-electron tunneling is influenced by electron–electron interaction. If occupation/unoccupation by a single electron in a quantum dot is viewed as a bit 1/0, we can say that the device can perform (N)AND and (N)OR operations simultaneously. Data input/output is performed by irradiation/absorption of photons. The (N)AND and (N)OR operations are performed by the relaxation of the electronic system to the (Fock) ground state which depends on the number of electrons in CQDs. When the device is constructed of semiconductor nanostructures, phonon emission from an electron is the main contributor to the energy dissipation process. We also present results of a theoretical analysis of the device performance. These results show that (i) the error probability at the final state depends on only the dissipation energy and becomes smaller as the dissipation energy becomes larger, and (ii) the speed of operation depends on the dissipation energy and dissipative interactions and becomes slower as the dissipation energy becomes larger if LA-phonon emission is taken into account. If the size of the dot is 10 nm, the speed of operation and the error probability are estimated to be about 10 ps and about 0.2 at 77 K, respectively. The basic idea of the device is applicable to two-dimensional (2D) pattern processing if the devices are arranged in a 2D array. © *1996 American Institute of Physics*. [S0021-8979(96)00501-X]

I. INTRODUCTION

The down-scaling of conventional large integrated circuits (LSIs) has two major problem areas—device physics problems and circuit architecture problems.[1] The most fundamental device physics problem relates to devices which operate under the condition in which many electrons can be treated as a continuous fluid, yet cannot operate properly when the down-scaling of the device causes a large statistical fluctuation in the number of electrons contributing to the operation. A possible method of overcoming this problem is to use the Coulomb interaction between electrons. As we observe in phenomena such as Coulomb blockade and the charging effect, the Coulomb interaction makes the fluctuation of the number of electron small and ultimately makes single-electron manipulation possible.[2] A single-electron transistor (SET),[3] a single-electron memory,[4] etc. have been proposed as applications of this phenomena, and operation has been experimentally confirmed at temperatures below 4 K. Such devices using Coulomb interaction have advantages in that the devices have no down-scaling limit and the operation remains robust as the device becomes smaller.

The problems in circuit architecture is that wiring needed for the integration of devices produces too much heat and causes a signal delay. It is, in principle, possible to construct quite dense circuits by integrating SETs using the conventional LSI architecture. However, as in the case of the conventional LSI, the problems of heat production and signal delay due to wiring remain. As an advance on conventional LSI architecture, a locally interconnected architecture and a cellular automata (CA)-like architecture have been proposed.

In 1987, Bate *et al*. first proposed such architectures.[1] The concept is essentially a 2D array of devices that couple with near neighbors. The coupling may be through short-wired interconnects or preferably by utilizing device–device interaction. Input/output (I/O) of data occurs at the periphery of the array. They showed an example of a system where the device (or cell) is a quantum dot (QD) and the coupling is electron tunneling between discrete levels. As more concrete examples of Bate's proposed architecture, Randall presented multi-gate-FET-type devices.[5] In these devices, a series of QDs is controlled by a third terminal added to each dot (called a ''quantum logic cell''). By switching the tunneling current through the cell, various binary-multi-input/one-binary-output logic functions become possible. Because coupling using tunneling is short range from the fabrication point of view, alternative coupling using long-range electrostatic interaction has been proposed. Bakshi *et al*. proposed a system where elongated quantum dots (called ''quantum dashes'') are arranged in a 1D/2D array.[6] They showed that the dipole moment in each dash is spontaneously polarized and the antiferroelectric phase appears. If a flip of dipole moments on individual dashes could be enforced, the resulting electrostatic perturbation would generate a ''domino''-type of response, flipping the dipole in the remaining dash, which is viewed as CA. Lent *et al*. elaborated on Bakshi's idea. Each cell consists of a central QD and four neighboring QDs occupied by two electrons, instead of a dash.[7,8] The cell has strong bistability of polarization. The polarization is encoded to the binary data, and the data is transferred by the intercell Coulomb interaction as in the quantum–dash array. In the Lent *et al*. concept, the I/O is delivered at the edge of the CA array (edge driven), and the ground state under the enforced input edge is regarded as the result of the computation (computing with the ground state).[9] They present the

[a]Electronic mail: knomoto@src.sony.co.jp

 0021-8979/96/79(1)/291/10/$6.00

arrays of AND gate, OR gate, NOT gate, etc., as concrete examples. The opt-electronic version of the CA architecture has been proposed by Teich *et al*.[10] They present a CA system which is an array of a subsystem (cell) consisting of a pair of coupled QDs occupied by a single electron. The subsystems are coupled via the dipole–dipole interaction. The temporal evolution of the system is optically controlled. They show a pair of subsystems can perform all the elementary logical operations, and a 1D array of the subsystems can perform some classes of 1D CA.

As another version of the device based on locally interconnected architecture, we will propose a novel AND/OR logic device which consists of a asymmetric coupled QD pair. We present only an early concept of the device in Ref. 11. In this article, we describe a general and essential concept of the device and give a theoretical analysis of the device performance in detail. The QDs are coupled by both tunneling and the Coulomb interaction. The device utilizes the difference between the one-electron ground state and the two-electron ground state for the operation. In other words, the electron-number-dependent (Fock) ground state is viewed as the result of operation. Although the way of preparing the system and I/O was not clear in the previous proposals, we propose a method of I/O using photon irradiation and absorption. We also discuss the effect of temperature and of the imperfection of the device quantitively.

This article is in the following order. We propose the structure of the device, the principle of operation, and the method of data I/O in Secs. II to IV. In Sec. V, we theoretically analyze the condition needed for the device operation, energy dissipation process (particularly photon or LA phonon emission process) needed for the operation, and discuss the relation among the dissipation energy, speed of operation, and error probability at finite temperature. In Sec. VI, we show that the device structure and the arrangement of the device units in 2D array reduces the error probability. The device also makes the high contrast read out. In Sec. VII, we discuss the subject related to the realization of the device and propose possible applications.

II. STRUCTURE

A cross section of the proposed device unit and its energy diagram are shown in Fig. 1. A type-II material system such as a InAs/AlSb heterostructure makes it possible to realize such a band structure. Other structural elements such as molecules can be also used. E_v is the valence band edge of a QD. E_{i0} and E_{i1} are respectively the lowest energy and the first excited energy of an electron strongly confined in the QD i. In order to selectively excite an electron in the QD i by a photon, the structure must be asymmetric and the relation $E_{10}>E_{20}$ must hold. U_i is the Coulomb energy when two electrons occupy the same QD i. A Schottky contact and a p-type ohmic contact are attached to the back and top of the device, respectively, to change the alignment of the energy levels by applying a bias between the QDs and to pull out or to put in holes. (We explain this in detail in the following section.) The electrodes have windows so that photons reach the QDs for I/O.

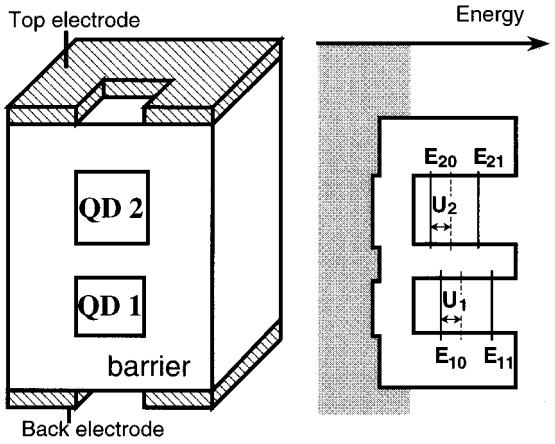

FIG. 1. The cross section of the device structure and energy diagram of the device when no bias is applied.

III. PRINCIPLE OF OPERATION: COMPUTING WITH FOCK GROUND STATE

We use a single electron within a QD as an information carrier and assign a bit $A_{\text{in } i}(A_{\text{out } i})=1/0$ to occupation/unoccupation of the QD i after input (at output). Here for simplicity, we restrict ourselves to zero temperature. The effect of finite temperature is discussed in the following section. Under the condition $\epsilon_{10}<\epsilon_{20}<\epsilon_{10}+U_1$ [see Fig. 2(b), where $\epsilon_{i0}=E_{i0}-e\phi_i$, ϕ_i is a scalar potential in the QD i], we assume that a single electron is selectivity input in the lowest energy level ϵ_{i0} in the QD i. The concrete method of

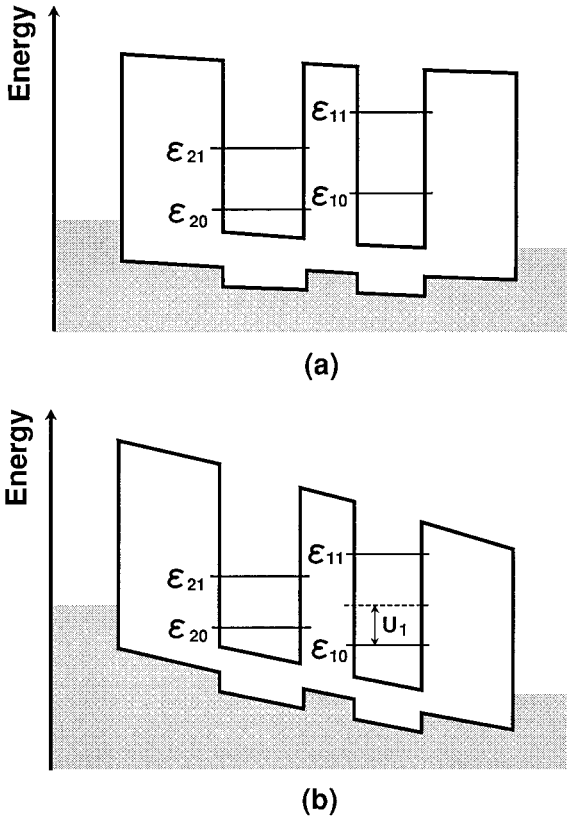

FIG. 2. The arrangement of the energy levels (a) when the first bit of information is input and (b) when the second bit of information is input.

TABLE I. The truth table of input and output.

Input		Output	
A_{in1}	A_{in2}	A_{out1}	A_{out2}
0	0	0	0
0	1	1	0
1	0	1	0
1	1	1	1

inputting an electron using light is discussed in the next section. If no electron is input in the lowest level ϵ_{10} in QD 1, an electron occupying the level ϵ_{20} in QD 2 decays to the level ϵ_{10} with dissipating energy due to spontaneous emission of a phonon or photon and finally stays in the one-particle ground state localized in QD 1. On the other hand, if an electron occupies level ϵ_{10}, an electron in level ϵ_{20} cannot tunnel into QD 1 due to Coulomb interaction and the electronic system stays in the two-particle ground state where each QD is occupied by an electron. We regard the final distribution of electrons as the result of operation $A_{\text{out } i}$. The $A_{\text{in/out } i}$ truth table is shown in Table I. From Table I, we know that the operations $A_{\text{out1}}=A_{\text{in1}}$ OR A_{in2} and, $A_{\text{out2}}=A_{\text{in1}}$ AND A_{in2} are realized simultaneously. If we exchange 0 for 1 in $A_{\text{in/out } i}$, the above operations of course become NOR and NAND.

Even at a finite temperature, if the difference between the first excited energy and the ground energy is much larger than the thermal energy, the principle of operation applies. (Detail will be discussed in Sec. V B.) We would like to emphasis that the dissipation of energy to an external reservoir is requisite for operation at a finite temperature, because the final output state must be stable under thermal fluctuation.

The essence of the operation of this device is to make use of the relaxation of the electron system to the ground state. In this sense, the operation is computing with the ground state, proposed by Lent *et al*.[9] However, there is an important difference between our idea and the idea of Lent *et al*. In the device proposed by Lent *et al*., operation is the relaxation to the ground states which depend on the boundary conditions of the edge in a fixed-number electron system. On the other hand, the ground states in our device which depend on the number of electrons with a fixed boundary condition is viewed as the result of the operation. Therefore, this is *computing with the Fock ground state*. From the architecture point of view, the computation is done by a two-cell CA in which a cell is a QD, the cell state is assigned by the occupation/unoccupation of an electron, and cell–cell coupling is Coulomb interaction and single-electron tunneling.

IV. INPUT, OUTPUT, AND RESET

Light (photon) irradiation is considered suitable for I/O, since it is difficult to make contact to each small QD by wiring. Furthermore, there is an advantage that light I/O makes parallel I/O possible. Here, we present an example of I/O by photon irradiation.

Input: We first input an electron into QD 1, then into QD 2. The first input of an electron into QD 1 is performed by exciting a valence-band electron in QD 2, then transferring the electron into QD 1. This can be done as follows. Initially, photons that have energy $\delta E_{\text{in}}=E_{20}-E_v$ are irradiated under the condition ($\epsilon_{10}>\epsilon_{20}$) shown in Fig. 2(a). When the photon is irradiated, the electron is excited to the level of ϵ_{20}, and the hole is absorbed by the top electrode. This prevents electron–hole recombination; the type-II material system enables this process. Next, bias between QDs is applied so that the condition $\epsilon_{10}<\epsilon_{20}<\epsilon_{10}+U_1$ is satisfied, and the electron in QD 2 is transferred into QD 1. (The reason we use such a complicated procedure to input an electron into QD 1 is that if we use photons whose energy is $E_{10}-E_v$ to excite an electron into QD 1, another electron is also excited into QD 2 because the band gap energy of QD 2 is smaller than that of QD 1.) The second electron is then input into QD 2 by irradiating the photons having energy δE_{in}. Note that when one electron has been already excited to the level ϵ_{20}, an additional electron at the level ϵ_{20} must have the energy of $\epsilon_{20}+U_2$. Therefore, only one electron can be excited in each QD.

Output: During reading out output of the device, the condition $\epsilon_{10}<\epsilon_{20}<\epsilon_{10}+U_1$ must be kept. The bit $A_{\text{out } i}$ may selectively be read out by irradiating photons that have energy $E_{i1}-E_{i0}$ and observing whether or not the photons are absorbed by the excitation of the electron in the QD i. Even if there are two electrons in the device, each electron absorbs photons independently at the high correlated limit $t \ll U_i$.[12]

Reset: To erase the electrons from the QDs, the bias has only to be set to zero. Then the holes come from the top electrode to the QDs and electron–hole recombination erase the electrons. Note that one can regard the emission/nonemission of the photons as the result of the logic operation. In fact, if the detection/nondetection of the photons is assigned $A_{\text{out}}=1/0$, the operation $A_{\text{out}}=A_{\text{in1}}$ OR A_{in2} is realized.

V. THEORETICAL ANALYSIS

A. Definition of "an electron in the QD"—The condition that an electron is localized in a QD

In this section, we define "an electron in the QD i" and show the condition in which the definition is valid. First, we consider the case in which there is one electron in the device, or CQD. We express the device by the following one-body model Hamiltonian H^c:

$$H^c=-\frac{\hbar^2}{2}\nabla\left(\frac{1}{m^*(\mathbf{r})}\nabla\right)+V_1(\mathbf{r})+V_2(\mathbf{r})-e\phi(\mathbf{r}). \quad (1)$$

Here $m^*(\mathbf{r})$ is the effective mass at the position $\mathbf{r}$. $V_i(\mathbf{r})$ is the potential energy when only the QD i exists. $\phi(\mathbf{r})$ is the scalar potential (bias voltage) at the position $\mathbf{r}$. We expand the ground state ψ_0 (eigenenergy E_0^c) and the first excited state ψ_1 (eigenenergy E_1^c) of H^c by the bonding state $(|1\rangle+|2\rangle)/\sqrt{2(1+\langle 1|2\rangle)}$ and the antibonding state $(|1\rangle-|2\rangle)/\sqrt{2(1-\langle 1|2\rangle)}$, where the state $|i\rangle\equiv\varphi_{i0}$ is the ground state of each QD, satisfying the Schrödinger equation:

$$\left[-\frac{\hbar^2}{2}\nabla\left(\frac{1}{m^*(\mathbf{r})}\nabla\right)+V_i(\mathbf{r})\right]\varphi_{\mathrm{in}}(\mathbf{r})=E_{\mathrm{in}}\varphi_{\mathrm{in}}(\mathbf{r}). \tag{2}$$

The result is given by

$$E^c_{1/0}=\epsilon^c\pm\frac{\Delta E}{2}, \tag{3}$$

$$\psi_{1/0}=\frac{1}{2}\sqrt{\frac{1}{\Delta E}}\left[\left(\mp\sqrt{\frac{(\Delta E+t_0)}{(1\mp S)}}+\Delta\epsilon_0\sqrt{\frac{(\Delta E+t_0)^{-1}}{(1\pm S)}}\right)|1\rangle\right. \tag{4}$$

$$\left.+\left(\sqrt{\frac{(\Delta E+t_0)}{(1\mp S)}}\pm\Delta\epsilon_0\sqrt{\frac{(\Delta E+t_0)^{-1}}{(1\pm S)}}\right)|2\rangle\right], \tag{5}$$

where

$$\epsilon^c=\frac{1}{2}\sum_{i\neq j}\left(E_{i0}+\frac{\langle i|\tilde{V}_j|i\rangle-S\langle j|\tilde{V}_j|i\rangle}{1-S^2}\right),$$

$$\Delta E=\sqrt{\Delta\epsilon_0^2+t_0^2}, \tag{6}$$

$$\Delta\epsilon_0=\frac{\epsilon_{20}-\epsilon_{10}}{\sqrt{1-S^2}},\quad t_0=\sum_{i\neq j}\frac{\langle j|\tilde{V}_j|i\rangle-S\langle i|\tilde{V}_j|i\rangle}{1-S^2}, \tag{7}$$

$$S=\langle 1|2\rangle,\quad \epsilon_{i0}=E_{i0}+\langle i|\tilde{V}_j|i\rangle,$$

$$\tilde{V}_i(\mathbf{r})=V_i(\mathbf{r})-e\phi(\mathbf{r}). \tag{8}$$

When (a) the overlapping between the wave function $|1\rangle$ and $|2\rangle$ is small ($S\ll 1$) and (b) energy difference $\Delta\epsilon_0$ between the one-body energy in each QD is much larger than the transfer energy $t(t\ll\Delta\epsilon_0)$, the eigenenergy and the eigenstate of the CQD becomes

$$E^c_0\sim\epsilon_{10},\quad \psi_0\sim|1\rangle,\quad E^c_1\sim\epsilon_{20},\quad \psi_1\sim|2\rangle \quad \text{for } \Delta\epsilon_0>0, \tag{9}$$

$$E^c_0\sim\epsilon_{20},\quad \psi_0\sim|2\rangle,\quad E^c_1\sim\epsilon_{10},\quad \psi_1\sim-|1\rangle \quad \text{for } \Delta\epsilon_0<0. \tag{10}$$

Thus, an electron is localized in each QD. Therefore, when conditions (a) and (b) are satisfied, we call the electron whose state ψ_i has large probability amplitude in the QD i "the electron in the QD i".

In order to deal with a one-electron channel and a two-electron channel in a unified way, we describe the device by the extended Hubbard-type Hamiltonian,[7,13]

$$H=\sum_{i\sigma}E^c_i a^\dagger_{i\sigma}a_{i\sigma}+\sum_i U_i n_{i\uparrow}n_{i\downarrow}+\frac{V}{2}\sum_{\substack{i,j\\ \sigma,\sigma'}}n_{i\sigma}n_{j\sigma'}, \tag{11}$$

where

$$n_{i\sigma}=c^\dagger_{i\sigma}c_{i\sigma}. \tag{12}$$

Here, E^c_i, U_i, and V are the one-body energy of the device, intradot Coulomb interaction and interdot Coulomb interaction, respectively. The operators $a^{(\dagger)}_{i\sigma}$ and $c^{(\dagger)}_{i\sigma}$ are, respectively, the annihilation (creation) operator of the spin-σ electron in the state ψ_i and φ_{i0}. We ignore the exchange Coulomb interaction because it is much smaller than U_i and V when $S\ll 1$. By making use of the identity:

$$\sum_{\substack{i\neq j\\ \sigma,\sigma'}}n_{i\sigma}n_{j\sigma'}+2\sum_i n_{i\uparrow}n_{i\downarrow}=N(N-1), \tag{13}$$

where

$$N=\sum_{i\sigma}n_{i\sigma}, \tag{14}$$

we obtain

$$H=\sum_{i\sigma}E^c_{i\sigma}a^\dagger_{i\sigma}a_{i\sigma}+\sum_i(U_i-V)n_{i\uparrow}n_{i\downarrow}+\frac{V}{2}N(N-1). \tag{15}$$

Once the system relaxes to a ground state, the total number of electrons N in the device does not change until reset is performed. So N can be treated as a constant after input and until output, and the last term is ignored for simplicity. By rewriting the operator $a_{i\sigma}$ in terms of the operator $c_{i\sigma}$, the above Hamiltonian can be reduced to the Hubbard-type Hamiltonian:

$$H=\sum_{i\sigma}\epsilon_i n_{i\sigma}+\sum_{i\neq j,\sigma}tc^\dagger_{i\sigma}c_{j\sigma}+\sum_i\tilde{U}_i n_{i\uparrow}n_{i\downarrow}, \tag{16}$$

where

$$\epsilon_i=\frac{\epsilon_{i0}}{1-S^2}, \tag{17}$$

$$t=\frac{1}{2(1-S^2)}\sum_{i\neq j}(SE_i+\langle j|\tilde{V}_j|i\rangle), \tag{18}$$

$$\tilde{U}_i=U_i-V. \tag{19}$$

By approximating the parameters up to the first order of S, the energy ϵ_i is equal to the one-body energy of an electron which is in the state $|i\rangle$, $\epsilon_{i0}=\langle i|H^c|i\rangle$, and the transfer energy t is equal to the off-diagonal matrix element $\langle i|H^c|j\rangle(i\neq j)$. Without calculating the exact form of eigenfunction, we easily know from the perturbation theory that the ground state of the electronic system of the device has a characteristic electron distribution depending on the parameters such as the separation between the energy levels in different QDs, $\Delta\epsilon\equiv\epsilon_2-\epsilon_1$, t, and $\tilde{U}$, as shown in Fig. 3. There is no definite boundary between the regions. In region I, if the inequality $t\ll|\Delta\epsilon|\ll\tilde{U}_i$ is satisfied, one electron is localized in the lower potential QD in the one-electron channel and two electrons are localized in each QD due to Coulomb interaction in the two-electron channel. Therefore the operation of the device is possible. On the other hand, in region II, if one electron occupies the device, its wave function extends in the whole device. Two electrons, however, are localized in each QD. In region III, the transfer energy is larger than both $|\Delta\epsilon|$ and $\tilde{U}_i$. So there is little correlation between electrons, and the electron wave function extends in the device. In region IV, electrons are localized in the lower potential QD in both the one-electron and two-electron channels. In this case, two electrons do not localize in each dot as

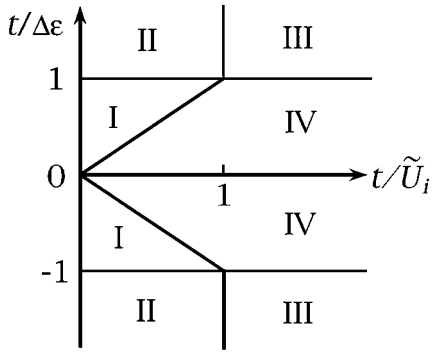

FIG. 3. Classification of the electron distribution of the ground state in the value of the parameters, the difference between the ground state energy levels in different QDs $\Delta\epsilon$, the transfer energy t and the Coulomb energy $\tilde{U}_i$. The device works in region I.

the result of two electrons being input. Therefore the device does not work. From the above discussion, we know that the condition for device operation is $t \ll |\Delta\epsilon| \ll \tilde{U}_i$. Because the energy difference $\Delta\epsilon$ can be controlled by applying bias between QDs, $\Delta\epsilon$ is not directly related to the structure of the device. The important condition that the device structure must satisfy is the condition $t \ll \tilde{U}_i$.

In the following discussion, to quantitatively estimate the conditions required for operation, the speed of the operation, error probability, etc., we assume that the shape of a single QD is a cube whose side length is $2a$. The QD is surrounded by a barrier whose height is V_0 in the z direction and infinity in the x,y direction. The QDs are arranged in the z direction at the spacing of $2d$. In other words, the potential $V_i(\mathbf{r})$ is given by $V_1(\mathbf{r})=V((x,y,z-a-d)$ and $V_2(\mathbf{r})=V(x,y,z+a+d)$, where $V(\mathbf{r})=+\infty$ for $|x|,|y|>a$, $V(\mathbf{r})=-V_0$ for $|x|,|y|,|z|<a$ and $V(\mathbf{r})=0$ for $|x|,|y|<a \cap |z|>a$. The scalar potential is given by $\phi(\mathbf{r})=Ez$ with the electric field E. The electron wave function $\varphi_{i0}(\mathbf{r})$ is assumed to be $\cos(\pi x/2a)\cos(\pi y/2a)\cos\{(k_w[z\pm(a+d)]\}$ in the QD and $\cos(\pi x/2a)\cos(\pi y/2a)\exp\{\pm k_b[z\pm(a+d)]\}$ in the barrier. The Coulomb energy U_i and V are respectively given by

$$U_i=\frac{e^2}{4\pi\epsilon}\int\int\frac{|\varphi_{i0}(\mathbf{r}_1)|^2|\varphi_{i0}(\mathbf{r}_2)|^2}{|\mathbf{r}_1-\mathbf{r}_2|}\,d\mathbf{r}_1\,d\mathbf{r}_2 \tag{20}$$

and

$$V=\frac{e^2}{4\pi\epsilon}\int\int\frac{|\varphi_{10}(\mathbf{r}_1)|^2|\varphi_{20}(\mathbf{r}_2)|^2}{|\mathbf{r}_1-\mathbf{r}_2|}\,d\mathbf{r}_1\,d\mathbf{r}_2. \tag{21}$$

We use the material parameters of InAs/AlSb ($m^*_{\mathrm{InAs}}=0.023m_0$, $m^*_{\mathrm{AlSb}}=0.12m_0$, $V_0=1$ eV, $\epsilon=14.6\epsilon_0$, where m_0 and ϵ_0 are the free electron mass and the dielectric constant of vacuum) for quantitative estimations.

The structure dependence of S and $t/\tilde{U}_i$ are shown in Figs. 4 and 5. Thus, if both the QD size and QD length are several 10 nm, the conditions (a) and (b) hold. A lithographic technique which can be used for such dimensions will be realized in the near future.

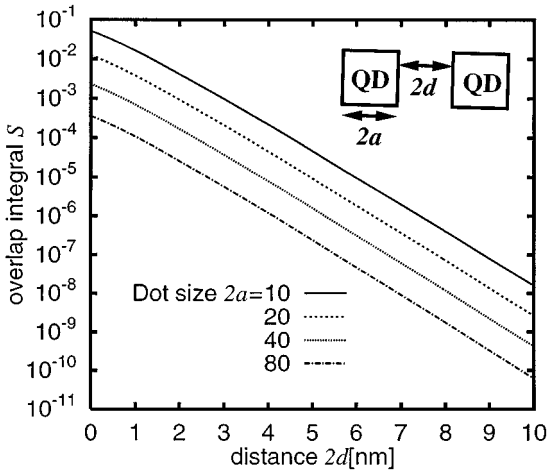

FIG. 4. Structure dependence of the overlapping integral S for the InAs/AlSb system. $2a$ and $2d$ denote the side of a QD and the distance between the different QDs, respectively.

B. Energy dissipation, speed of operation, and error probability—LA phonon, photon scattering in CQD

In this section, we estimate the operating speed and the error probability by taking the phonon and photon emission process into account, and we also discuss the relation among dissipation energy, speed of operation, and error probability.

Since the ground state is viewed as the result of operation in the present device, the transition from the excited state to the ground state with dissipating energy corresponds to the operation. Here, the excited energy is the state in which an electron is input in QD 2 (ψ_1) and the ground state is the state in which an electron occupies QD 1 (ψ_0). If the device consists of semiconductors, energy dissipation occurs when phonons or photons are emitted from electrons. The rate at which this process occurs determines the speed of operation. (Of course, it takes time to perform I/O. The time, however, depends on the I/O method. Here for simplicity, we will focus on only the time required for an electron to relax.)

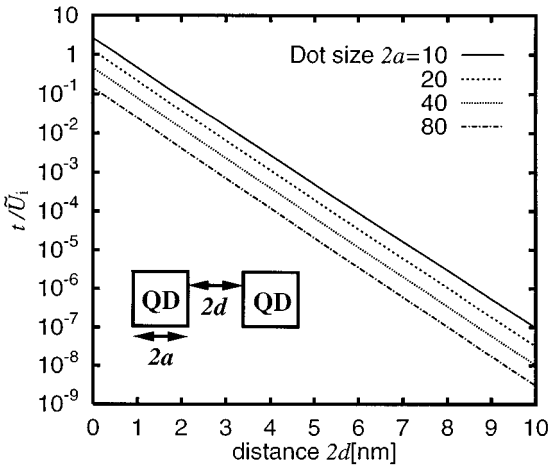

FIG. 5. Structure dependence of the ratio of the transfer energy t to Coulomb energy $\tilde{U}_i$ for the InAs/AlSb system. $2a$ and $2d$ denote the side of a QD and the distance between the different QDs, respectively.

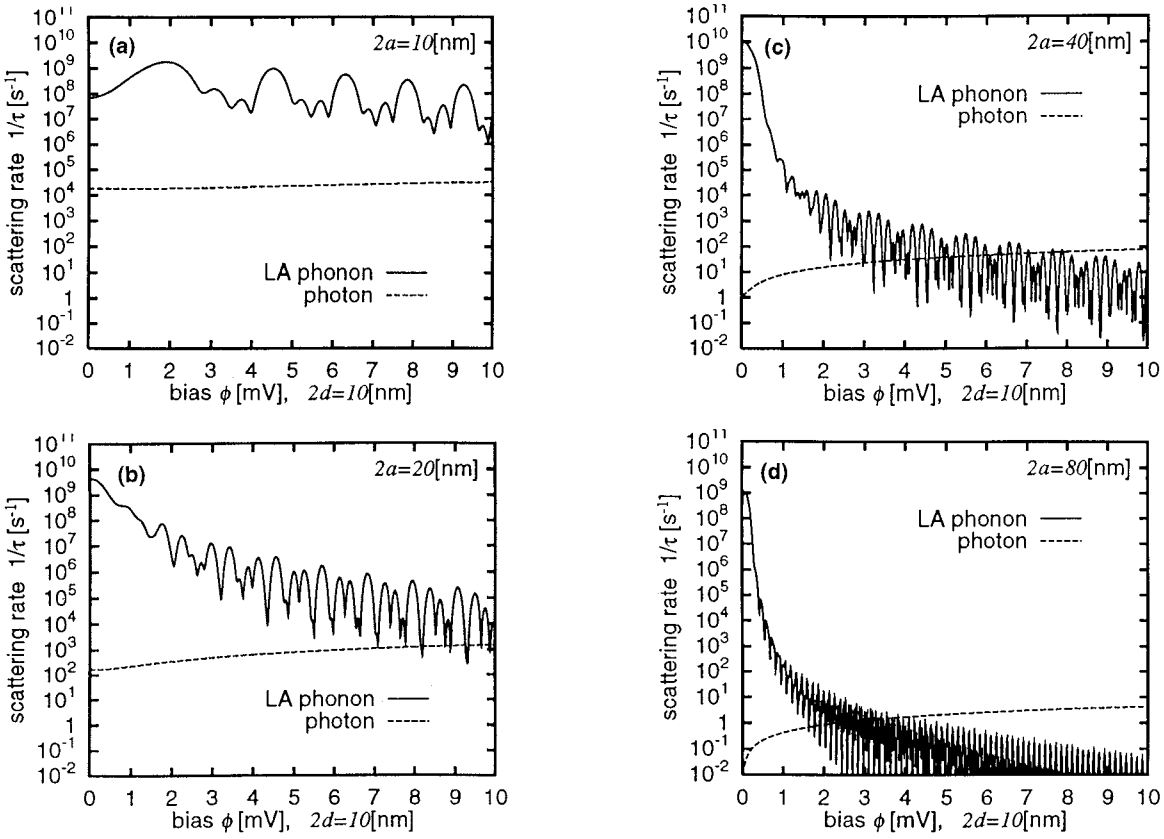

FIG. 6. The electron scattering rate at $T=0$ K due to emission of LA phonons or photons in CQDs where the distance between QDs is $2d=10$ nm and (a) the side of a QD is $2a=10$ nm, (b) $2a=20$ nm, (c) $2a=40$ nm and (d) $2a=80$ nm. ϕ denotes the bias voltage applied between QDs.

The speed of operation $\tau^{-1}(\Delta E)$ where ΔE is the dissipation energy of an electron can be estimated with the first-order perturbation formula using Fermi's golden rule,

$$\tau^{-1}_{\text{em./abs.}}(\Delta E)=\frac{2\pi}{\hbar}\sum_{\mathbf{q}}|M^{10}_{\mathbf{q}}|^2\delta(\Delta E\pm\hbar\omega_{\mathbf{q}})\left[n_q(T)+\frac{1}{2}\pm\frac{1}{2}\right]. \tag{22}$$

Here the upper (lower) sign denotes the emission (absorption) of a phonon or photon. $n_q(T)$ is the Bose–Einstein distribution function, $n_q(T)=[\exp(\hbar\omega_q/k_BT)^{-1}]^{-1}$, where T is the phonon or photon temperature and $\hbar\omega_q$ is the energy of the phonon or photon with wave vector $\mathbf{q}$.

In a high-dimensional system, e.g., quantum wells, the dominant relaxation process is longitudinal-optical (LO) phonon emission via Fröhlich interaction, with a subpicosecond relaxation time. In the QD system, however, this process is forbidden due to the discrete nature of the levels, unless the level separation equals the LO phonon energy $\hbar\omega_{\text{LO}}$. (We define $\hbar\omega_{\text{LO}}$ as energy of the zero-frequency LO phonon.) So, in a system, longitudinal-acoustic (LA) phonon emission process via deformation potential interaction—which is weak in the bulk compared to Fröhlich interaction—is the main contributor to the relaxation process, since the LA phonon has continuous spectra from zero to several 10 meV.

When considering the LA phonon, we cannot use the dipole approximation $e^{i\mathbf{q}\cdot\mathbf{r}}\simeq 1$, because in a QD with the size of about 10 nm, the wavelength of an LA phonon interacting with an electron becomes about 10 nm, which is comparable to the extent of the electron wave function. On other hand, for the electron–photon interaction the dipole approximation is valid, because the wavelength of the photon interacting with the electron in a QD is several 100 μm.

Based on the above discussion, we calculate the matrix element $M^{10}_{\mathbf{q}}$ given by

$$M^{10}_{\mathbf{q}}=\begin{cases} D\sqrt{\dfrac{\hbar q}{2\rho v_s V}}\,\langle\psi_0|e^{\mp i\mathbf{q}\cdot\mathbf{r}}|\psi_1\rangle & \text{for LA-phonon scattering} \quad (23)\\ ie\sqrt{\dfrac{\hbar cq}{2\epsilon V}}\,\langle\psi_0|z|\psi_1\rangle & \text{for photon scattering,} \quad (24)\end{cases}$$

where V is the system volume, each parameter for InAs is the deformation potential $D=-6$ eV, the density $\rho=5.7\times10^3$ kg/m^3, and the sound velocity $v_s=2.7\times10^3$ m/s. For the LA phonon, we assume a linear dispersion relation $\hbar\omega_q=\hbar v_s q$. Ignoring the confinement effect of the phonon modes is known to be legitimate for the LA phonon.[14] Using these parameters, $\tau^{-1}_{\text{em.}}$ is numerically calculated as shown in Fig. 6 at $T=0$ K. The main contributor to the decay of an electron is LA-phonon emission. The decay time becomes 10^{-9} to 10^{-6} s. The rate of LA-phonon emission decreases with respect to the dissipation energy in a series of oscillations of decreasing amplitude. At finite temperatures, though the rate increases in the overall range of energy due to the stimulated emission, the pattern of oscillation does not change. These results are similar to the rate of emitting an LA phonon from

an electron in a single QD, which was calculated by Bockelmann and Bastard.[15] Such behavior arises from the fact that as the dissipation energy increases, the wavelength of the phonon decreases and the matrix element $M_{\mathbf{q}}^{10}$ decreases with the oscillations due to the rapid oscillation of the factor $e^{\pm i\mathbf{q}\cdot\mathbf{r}}$. Rapid oscillation occurs only when the size of the electron wave function is comparable to the wavelength of the interacting system such as the LA-phonon system. On the other hand, the factor $e^{\pm i\mathbf{q}\cdot\mathbf{r}}$ is ~ 1 for electron–photon interaction and such oscillation does not occur. The reason the relaxation time is longer for a larger QD is that the electron wave function is strongly localized in a larger QD, so the overlap between the wave function ψ_0 and ψ_1 becomes smaller.

In this calculation, we take only LA phonon and photon scattering into account for the relaxation process. In a real material system, however, there are many other scattering processes, such as interface–phonon scattering and folded-LO phonon scattering. We believe, therefore, that the relaxation time of 1 ns–1 μs is the maximum time and that relaxation in a real device occurs faster than our estimated time.

As mentioned above, the operating speed of the device strongly depends on the dissipation energy. In order to realize faster operations, the dissipation energy must be reduced by lowering the applied bias voltage between dots. If the dissipation energy is reduced to speed up the operation, the error probability of the operation increases. This is because an electron in the ground state is easily excited by a heat bath to the first or higher excited state at a finite temperature. The error probability is equal to the probability that the electron system takes an excited state. The probability is estimated by calculating the temporal evolution of the electron system including dissipation processes. However, the quantum mechanical evolution of the whole system including phonons and photons is extraordinarily complicated. So we ignore the quantum interference effect and use the following two-level rate equation. (Here we use an approximation in which the difference between the first excited energy and the second excited energy is much more than the thermal energy k_BT. This condition can be realized by optimizing the device structure.)

$$\frac{dn_2}{dt} = -\frac{n_2}{\tau_{\text{em.}}} + \frac{n_1}{\tau_{\text{abs.}}}, \quad n_1(t) + n_2(t) = 1, \tag{25}$$

where n_i is the expected value of the number of electron occupying the QD i. If we assume that an electron is input into QD 2 at the time $t=0$, the error probability $p_{\text{error}}(t)$ at the time t is given by $n_2(t)$ and becomes

$$p_{\text{error}}(t) = n_2(t) = \frac{1}{1+\exp(\beta\Delta E)} + \exp(-t/\tau)\,\frac{1}{1+\exp(-\beta\Delta E)}, \tag{26}$$

where

$$\frac{1}{\tau} = \frac{1}{\tau_{\text{em.}}} + \frac{1}{\tau_{\text{abs.}}}, \quad \beta = \frac{1}{k_BT}. \tag{27}$$

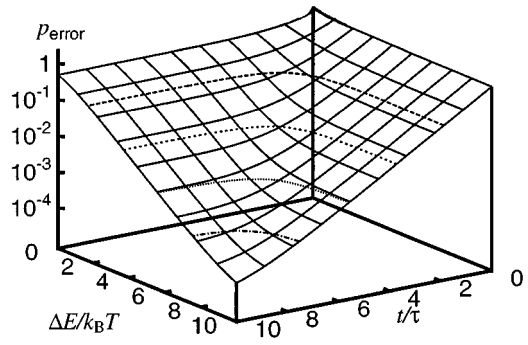

FIG. 7. Error probability p_{error} as a function of the dissipation energy E normalized by the thermal energy k_BT and the time t normalized by the relaxation time τ.

We show the dimensionless time t/τ dependence and the dimensionless dissipation energy dependence $\beta\Delta E$ of the error probability p_{error} in Fig. 7. From Eq. (26), we know that p_{error} decreases exponentially with the time constant τ and eventually becomes constant. At $t=\infty$, the error probability p_{error} coincides with the probability that the system is in a excited state in a thermal equilibrium state which has the same temperature as the heat bath. If all the excited states are taken into account, the error probability becomes $p_{\text{error}} = 1 - e^{-\beta E_0}[\text{Tr}(e^{-\beta H})]^{-1}$, where H is the electronic Hamiltonian and E_0 is the ground-state energy of the electron system. These statements are restricted to not only our device but also to all devices based on "computing with the ground state".[9] Since it is useless if the output is obtained in a finite time, the output must be done before the system reaches thermal equilibrium. For example, if the conditions $\beta\Delta E > 10$ and $t/\tau > 10$ are satisfied, the error probability is less than 10^{-4}.

The present device, the maximum dissipation energy is $\Delta E = \tilde{U}/2$. From this value, the relation between the device size and the error probability can be estimated. We show the error probability in the thermal equilibrium state in Fig. 8. When the size of the dot is 10 nm, the maximum dissipation energy becomes about 10 meV and the error probability turns out to be less than $O(10^{-3})$ $[O(10^{-1})]$ at a temperature of

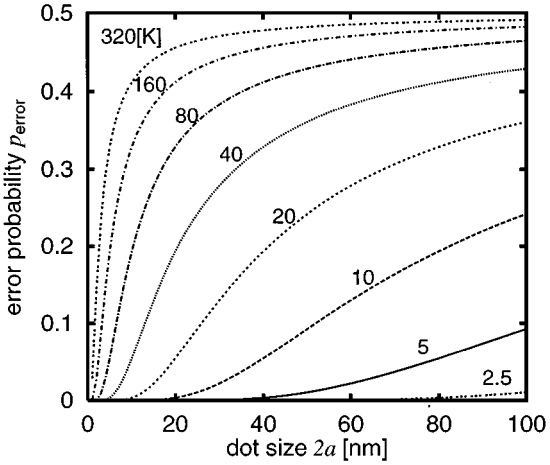

FIG. 8. Error probability p_{error} at the operation time $t=\infty$ as a function of the side of a QD $2a$ and the operation temperature for the InAs/AlSb system.

lower than 20 K (77 K). Thus operation at higher temperatures is difficult. This is because it is difficult to make $\tilde{U}$ large by down-sizing a QD. One possible method of raising the operation temperature is to employ material having a lower dielectronic constant. Another method is to use multiple devices to represent one bit of information. As discussed in the following section, the latter method can be introduced quite naturally by performing I/O using light.

VI. REDUCTION OF ERROR PROBABILITY AND HIGH-CONTRAST READOUT USING AN ARRAY OF DEVICE UNITS

As discussed in Sec. IV, we consider that the method using light is suitable for I/O. In this case, the size of an information unit is restricted by the wavelength of light. For instance, if a cubic InAs QD whose side of several 10 nm is used, the energy of the photon used for I/O becomes several 100 meV (which is nearly equal to the value $E_g^{\mathrm{InAs}} + 3\hbar^2\pi^2/[2m^*_{\mathrm{InAs}}(2a)^2]$, where E_g^{InAs} is the band gap energy of InAs (0.36 eV) for inputting and nearly equal to the value $3\hbar^2\pi^2/[4m^*_{\mathrm{InAs}}(2a)^2]$ for outputting). The corresponding wavelength of the energy is several μm. Therefore the area of an information unit becomes about 1 $\mu\mathrm{m}^2$. In this case, the whole device structure in which multiple device units carry an information unit is realized. For example, if device units with a size of 10 nm are arranged in a 2D square lattice with spacing of 0.1 μm, and if 100 such layers are stacked by shifting by one device unit, the face perpendicular to the stacking direction seems to be filled by device units with a density of 10^4 units/$\mu\mathrm{m}^2$. This structure has the following advantages: (i) The error probability of an information unit is reduced considerably compared to that of a device unit, (ii) by arranging the device units densely, which is equivalent to enlarging the absorption cross section of photons, we can read out output in high contrast.

(i) Reduction of the error probability. Here the error is defined as being caused when more than n device units of N device units work incorrectly. If we write the error probability of an device unit as p_{error}, the error probability of an information P_{error} is given by

$$P_{\mathrm{error}} = \sum_{k=n}^{N} {}_N C_k p_{\mathrm{error}}^k (1-p_{\mathrm{error}})^{N-k}. \tag{28}$$

As shown in Fig. 8, $p_{\mathrm{error}} \simeq 0.2$ for InAs QD with a size of 10 nm at 80 K. In this case, if $N=1000$ and $n=250$ (500), the error probability of $P_{\mathrm{error}} \simeq 7\times10^{-5}$ (4×10^{-99}) is realized. Thus representing an information unit by many device units makes it possible to reduce the error probability of an information unit.

(ii) High-contrast read out. In order to read out an electron in a QD by the absorption of photons, the electron is excited by the absorption of a photon and the electron must decay through a nonradiative process such as emission of phonons. Because overlapping between electron wave functions localized in the same QD is larger than that in different QDs, the nonradiative process mainly occurs within a single QD. So its dissipation energy of several 100 meV due to the nonradiative process can be larger than the energy $\hbar\omega_{\mathrm{LO}}$. If the dissipation energy is around $\hbar\omega_{\mathrm{LO}}$, multiphonon emission process (particularly an LO$\pm$LA process) becomes important, as was discussed by Inoshita and Sakaki.[16] The rate of phonon emission is estimated to be about 10^{10}/s. On the other hand, the rate of photon emission is estimated to be about 10^6/s. This means that most of the photons irradiated to the device unit will be absorbed. Of course, photons irradiated to the open space between device units are not absorbed. Therefore, the ratio of the device-unit area to the total area determines the absorption rate. If we fill the face which is normal to the direction of irradiation with device units, most of the photons will be absorbed and high-contrast readout becomes possible.

VII. DISCUSSION

We discuss several subjects related to the realization of the device.

A. Size fluctuation

Using only current structuring techniques (e.g., electron-beam lithography), it may be impossible to fabricate thousands of device units without size fluctuation. It is necessary, therefore, to determine the tolerance of the size fluctuation. The size fluctuation causes two kinds of errors—the operation error and I/O error.

First, we discuss the operation error caused by size fluctuation. Size fluctuation ΔL causes one-body energy fluctuation ΔE which is approximately given by $\Delta E \sim \hbar^2\pi^2/(2m^*L^2)(\Delta L/L)$, where L is the side of a QD. The energy fluctuation ΔE changes the difference $\Delta\epsilon$ between the ground state and the first excited energy in each device. To obtain the desired electron distribution of the ground state, ΔE must be smaller than $|\Delta\epsilon|$. As shown in Sec. V A, the inequality $|\Delta\epsilon| \ll \tilde{U}$ must be satisfied. So ΔE must also be much smaller than the Coulomb energy $\tilde{U}$. Therefore, the tolerance of size fluctuation is given by

$$\frac{\hbar^2}{2m^*}\left(\frac{\pi}{L}\right)^2 \frac{\Delta L}{L} \ll \tilde{U}. \tag{29}$$

Using the approximation $\tilde{U} \simeq e^2/(4\pi\epsilon L)$, the inequality is rewritten by

$$\Delta L \ll \frac{e^2}{4\pi\epsilon}\frac{2m^*}{\hbar^2\pi^2} L^2. \tag{30}$$

Thus the size tolerance ΔL for a larger QD becomes larger. When a QD is constructed of InAs with, for example, $L=10$ (100) nm, the size tolerance becomes $\Delta L \ll 0.6$ (60) nm. However, when a larger QD is used, the error probability becomes larger due to thermal fluctuation, even if the size of the device does not fluctuate. Thus, it turns out that the one-monolayer control in the fabrication process is required for devices which work at several 10 K. On the other hand, if the device is used at a temperature below several Kelvin, size fluctuation can be limited to about 10 nm, which can be achieved by today's advanced fabrication technology.

Next we discuss the I/O error due to size fluctuation. In order to selectively read out the existence of an electron in different QDs, the energy difference between $E_{11}-E_{10}$ and

$E_{21}-E_{20}$ must be larger than the one-body energy fluctuation ΔE. The tolerance of the size fluctuation ΔL is given by

$$\Delta L_i < \left| \left(\frac{L_i}{L_1}\right)^2 - \left(\frac{L_i}{L_2}\right)^2 \right| L_i , \tag{31}$$

where L_i is the side of the QD i. Thus, when the difference between L_1 and L_2 is increased, the tolerance increases. Because we can determine L_1 and L_2 independently, we cannot give a definite value for ΔL_i. For example, if $L_1/L_2=0.9$ and $L_1=10$ (100) nm, the condition $\Delta L_1<1.9$ (19) nm, $\Delta L_2<2.6$ (26) nm must hold for I/O.

If we use a monochromatic light for I/O, we can access only the device units which resonate with only one frequency of the light. If such accessible devices are few, we cannot a obtain detectable signal from the device units. However, if we use light which has finite bandwidth $\Delta\omega$, satisfying the condition $\Delta E<\hbar\Delta\omega<|(E_{11}-E_{10})-(E_{21}-E_{20})|$, such I/O errors do not occur.

B. Impurities and defects

The present device utilizes a single electron as a bit of information and utilizes single-electron tunneling between 0D-quantized levels. If an impurity or an defect exist in the device unit, an electron is unintentionally input into a QD and/or the way of alignment of the discrete energy levels changes. In such a case, the device no longer operates. In particular, conventical lithography using electron-beam lithography and etching causes many defects at the etched surface due to damage during etching or due to some contamination in the environment. Therefore *in situ* nondamage fabrication technique must be improved to realize this device.

C. Thermal excitation of electrons form a valence band level

At a finite temperature, photons or phonons in reservoirs excite electrons from a valence band level into an unoccupied conduction band level, which is ignored in the above discussion. This unintentional input of electron into a QD also causes errors in operation. When no bias is applied to the device, this thermally excited electron immediately recombines with a hole and thermal equilibrium is realized. In bulk InAs, the intrinsic carrier density at 300 (77) K is about 8×10^{14} (5×10^{5})/cm^3. This corresponds to only 8×10^{-4} (5×10^{-13}) electrons in a cube with a side of 10 nm. If the QD structure is fabricated, the effective band gap becomes large compared to that in the bulk, so carrier density decreases. (Here we assume that the Fermi energy changes little with the QD structure.) Therefore, the assumption that no electron is in a QD is legitimate. However, when bias is applied, the thermally excited electron and hole separate spatially. In this case, the electron cannot disappear from the conduction band level, since electron–hole recombination cannot occur. Therefore the problem is whether or not an electron is thermally excited through the operation process: input–electron relaxation–output (readout).

In the following, we compare thermal excitation time and operation time. For direct semiconductors with a large band gap, the time scale of excitation is determined by optical excitation. The time scale $\tau_{c,v}^{\text{opt.}}$ is estimated by the first-order perturbation formula:

$$\tau_{c,v}^{\text{opt.}^{-1}} = \frac{\omega_q e^2}{8\pi^2\epsilon_0\hbar m_0^2 c^3}\, n_q(T) \int |M_{c,v,\mathbf{q}}^{\text{opt.}}|^2 d\Omega ,$$
$$M_{c,v,\mathbf{q}}^{\text{opt.}} = \langle c|e^{i\mathbf{q}\cdot\mathbf{r}}\mathbf{e_q}\cdot\mathbf{p}|v\rangle , \quad n_q(T)=\frac{1}{e^{\hbar\omega_q/k_BT}-1} , \tag{32}$$

where ω_q denotes the resonant transition frequency between the initial and final state and $\mathbf{e_q}$ denotes the polarization vector of the light mode with momentum $\mathbf{q}$. The one-particle wave function $|c(v)\rangle$ of an electron at the conduction (valence) band edge is approximately given by the product of a envelope function $|\psi_{c(v)}\rangle$ and the Bloch function at the conduction (valence) band edge $|u_{c(v)}\rangle$: $|c(v)\rangle=|\psi_{c(v)}\rangle|u_{c(v)}\rangle$. Using the inequality $|\langle\psi_c|\psi_v\rangle|\leq 1$ and the dipole approximation $e^{i\mathbf{q}\cdot\mathbf{r}}\simeq 1$, the matrix element $M_{c,v,\mathbf{q}}^{\text{opt.}}$ is calculated as

$$|M_{c,v,\mathbf{q}}^{\text{opt.}}|^2 \leq |\langle u_c|\mathbf{e_q}\cdot\mathbf{p}|u_v\rangle|^2 . \tag{33}$$

For III–V semiconductors,[17]

$$|\langle u_c|\mathbf{e_q}\cdot\mathbf{p}|u_v\rangle|^2 \simeq \frac{m_0^2 E_g(E_g+\Delta)}{12m^*(E_g+2\Delta/3)} , \tag{34}$$

where Δ is the spin orbit splitting. As a result, the maximum excitation rate becomes

$$\tau_{c,v}^{\text{opt.}^{-1}} \leq \frac{\omega_q e^2}{24\pi\epsilon_0\hbar m^* c^3}\,\frac{E_g(E_g+\Delta)}{E_g+2\Delta/3}\, n_q(T) . \tag{35}$$

When $\hbar\omega_q=E_g$ and using material parameters for InAs (e.g., $E_g=0.36$ eV, $\Delta=0.38$ eV), we get

$$\tau_{c,v}^{\text{opt.}^{-1}} \leq 2\times10^7[\text{s}^{-1}]\, n_q(T) ,$$
$$n_q(T)=\frac{1}{\exp(0.36[\text{eV}]/k_BT)-1} . \tag{36}$$

When the temperature is 300 (77) K, the time $\tau_{c,v}^{\text{opt.}}$ becomes 5×10^{-2} (1×10^{16}) s. On the other hand, the operation time is the sum of the time for I/O and electron relaxation. Since the time for the I/O using light is shorter than picoseconds, the operation time is dominated by the time for electron relaxation of 10^{-9}–10^{-6} s. So the thermal excitation time is significantly longer than the operating time. Therefore, we obtain results before excitation occurs. The thermal excitation of an electron in the valence band level does not degrade the device performance.

D. 2D pattern processing

If we irradiate the 2D patterns to the 2D array of the present device units, each device unit performs the AND/OR operation in parallel, which makes the high-speed 2D pattern AND/OR operation possible. However, to achieve the universal computation the operation NOT and the propagation of the data to the following device must be realized. These are subjects for future investigation.

E. Frequency-domain processing

It is extremely difficult to make thousands of QDs homogeneous. The fact that there is inhomogeneity in the size of QDs means that we can use various frequencies of light for I/O. If we assign the address of binary data of one-dimensional information to the frequency of I/O, the AND/OR operation is done in each unit of information addressed by the frequency. This method is analogous to the operation of optical memories based on persistent spectral-hole burning (PHB).[18] The present device is not mere memory, but functional memory.

Since this method makes use of inhomogeneity in the size of QDs, we apply quantum size (self-assembled) dots grown by Stranski–Krastanow growth mode using molecular beam epitaxy (MBE)[19] to the fabrication process.

VIII. SUMMARY

We have proposed a novel logic (AND/OR) device using a pair of CQD. In this device, occupation/unoccupation by a single electron in a QD is viewed as a bit 1/0. The essence of the operation of this device is that electron(s) input in the CQD spontaneously relax to the ground state depending on the number of electrons in the CQD—computing with the Fock ground state. The energy of an electron is dissipated mainly by LA-phonon emission. The emission rate determines the speed of operation. The rate decreases in a series of oscillations with respect to the dissipation energy and the value estimated to be 10^9 to 10^6 s^{-1}. The error rate p_{error} of the device unit decreases with respect to the dissipation energy, which is independent of the dissipation process. When the energy of dissipation becomes 10 meV, which is a typical dissipation energy when a cubic InAs QD with a size of 10 nm is used, the error rate p_{error} becomes 0.2 (10^{-3}) at 80 (20) K.

We have also shown that constructing an information unit by a 2D device unit array makes it possible to reduce the error probability of an information unit and to read out the output in high contrast. The I/O of the 2D pattern to/from the 2D device unit array makes parallel and therefore high-speed pattern processing possible.

As the principle of the present device, the idea that data processing is performed by electrons (Fermions)—whose Coulomb interaction coupled with the Pauli exclusion principle give rise to nontrivial functions—and that the data I/O are performed by photons (Bosons)—which eliminate wiring to each device unit for I/O—could lead to a new device architecture.

ACKNOWLEDGMENTS

We would like to to thank K. Taira for encouragement and fruitful discussions. This work was performed under the management of FED as a part of the MITI R&D program (Quantum Functional Devices Project) supported by NEDO.

[1] R. T. Bate, G. A. Frazier, W. R. Frensley, J. W. Lee, and M. A. Reed, Quant. Wells Superlatt. Phys., SPIE **792**, 26 (1987).
[2] *Single Charge Tunneling*, edited by H. Grabert and M. H. Devoret (Plenum, New York, 1992).
[3] M. A. Kastner, Rev. Mod. Phys. **64**, 849 (1992).
[4] K. Nakazato, R. J. Blaikie, J. R. A. Cleaver, and H. Ahmed, Electron. Lett. **29**, 384 (1992).
[5] J. N. Randall, Nanotechnology **4**, 41 (1993).
[6] P. Bakshi, D. A. Broido, and K. Kempa, J. Appl. Phys. **70**, 5150 (1991).
[7] C. S. Lent, P. D. Tougaw, and W. Porod, Appl. Phys. Lett. **62**, 714 (1993).
[8] C. S. Lent and P. D. Tougaw, J. Appl. Phys. **74**, 6227 (1993).
[9] C. S. Lent, P. D. Tougaw, W. Porod, and G. H. Berstein, Nanotechnology **4**, 49 (1993).
[10] W. G. Teich, K. Obermayer, and G. Mahlar, Phys. Rev. B **37**, 811 (1988).
[11] K. Nomoto, R. Ugajin, T. Suzuki, and I. Hase, Electron. Lett. **29**, 1380 (1993).
[12] R. Ugajin, Phys. Rev. B **51**, 11136 (1995).
[13] R. Ugajin, T. Suzuki, K. Nomoto, and I. Hase, J. Appl. Phys. **72**, 1041 (1994).
[14] M. V. Klein, IEEE J. Quantum Electron. **QE-22**, 1760 (1986).
[15] U. Bockelmann and G. Bastard, Phys. Rev. B **42**, 8947 (1990).
[16] T. Inoshita and H. Sakaki, Phys. Rev. B **46**, 7260 (1992).
[17] E. O. Kane, J. Phys. Chem. Solids **1**, 249 (1957).
[18] G. Castro, D. Haarer, R. M. Macfarlane, and H. P. Trommersdorff, U.S. Patent No. 4,101,976 (July 18, 1978).
[19] D. Leonard, M. Krishnamurthy, C. M. Reaves, S. P. Denbaars, and P. M. Petroff, Appl. Phys. Lett. **63**, 3203 (1993).